

PROTON EXCHANGE MEMBRANE FUEL CELL MODELLING USING MOVING LEAST SQUARES TECHNIQUE

R. Tirnovan¹, S. Giurgea², A. Miraoui²

1 – Technical University of Cluj-Napoca, Romania

2 - University of Technology of Belfort-Montbéliard, France

Abstract - Proton exchange membrane fuel cell, with low polluting emissions, is a great alternative to replace the traditional electrical power sources for automotive applications or for small stationary consumers. This paper presents a numerical method, for the fuel cell modelling, based on moving least squares (MLS). Experimental data have been used for developing an approximated model of the PEMFC function of the current density, air inlet pressure and operating temperature of the fuel cell. The method can be applied for modelling others fuel cell sub-systems, such as the compressor. The method can be used for off-line or on-line identification of the PEMFC stack.

Keywords: fuel cell, model, moving least squares, approximation

1. INTRODUCTION

Pollution is nowadays one of the most important problems, to face up. One of the solutions is the use of clean energy sources, which result in no carbon oxide emissions. Among them, fuel cell systems, depending on the hydrogen production technology, can be clean energy and renewable energy sources. They use hydrogen as fuel and oxygen as oxidant and they are more receiving attention ever increasingly since they can store energy and release it without polluting by-products (Blunier, *et al.*, 2007).

Fuel cells power generating systems represent a solution to replace traditional power sources because of their high efficiency and multiple applications (transportation applications, stationary applications, portable applications).

Fuel cell based power plants are currently under rapid development and first plants are expected by the next few years with size ranging from few kW up to 1 MW (Cogeneration & On-Site Power Production, 8, Issue 1 January/February 2007, News).

In particular, Proton Exchange Membrane Fuel Cells (PEMFC) are most suitable for automotive applications because of their low temperature that allows a fast start-up, because of their high power density, which ensures excellent power/volume ratio.

Over the last decades, many PEMFC models, either theoretical or empirical, have been described in literature. These models can be categorized as follow (Cheddie, *et al.*, 2005; Kim, *et al.*, 1995):

- analytical models - many simplifying assumptions are made about the variables in the cell for developing an approximate relationship between the voltage and the current density. They can be useful if quick calculations are required for simple systems or for control applications;
- mechanistic models - differential and algebraic equations are derived based on the physics and electro-chemistry of the phenomena within the cell. Mechanistic models can be subcategorized as multi-domain models or single domain (or unified) models;
- semi-empirical approaches - theoretically derived differential and algebraic equations with

empirically determined relationships. Empirical relationships are employed when the physical phenomena are difficult to model or the theory of the phenomena is not well understood;

- empirical approaches – these models are based on experimental data and mimic as well as is possible the real behaviour of the system.

This paper discusses a numerical method for modelling the fuel cell (FC) based on the MLS. It starts from the experimental dataset presented in ref (Kim, *et al.*, 1995). The dataset is given for stationary conditions for a PEMFC supplied with hydrogen and air, and it gives measured cell voltage $V_i(J,p,T)_{i=1...N}$ as function of the current density J , the air pressure p and the operating FC temperature T , with N the number of the experimental points. These experimental points are represented in Fig.1 for two temperatures (50 °C and 70 °C). Python language has been used to implement the proposed PEMFC model.

2. THE PROPOSED METHOD DESCRIPTION

2.1. Context

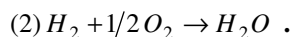
An element of fuel cell carries out the direct transformation of the chemical energy of a reaction (the change in the free Gibbs energy of reaction) into electric power according to the equation (Blunier, *et al.*, 2007):

$$(1) \Delta G + nF \cdot E_{eq} = 0 \quad \text{where} \quad \Delta G < 0 ,$$

with:

- E_{eq} – electromotive force (e.m.f) of the stack to balance;
- n – the number of the electrons exchanged in the elementary electrochemical reactions;
- $F= 96500$ C, Faraday constant.

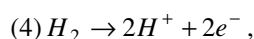
In the case of the hydrogen/oxygen stack, the total chemical reaction, associated with this transformation, is the combustion of hydrogen in oxygen:



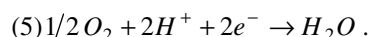
It corresponds, for standard conditions, with an e.m.f. to the balance at 25 °C:

$$(3) E_{eq}^0 = -\frac{\Delta G^0}{nF} = \frac{237 \times 10^3}{2 \times 96\,500} = 1.229 \text{ V} .$$

The electrochemical oxidation of hydrogen is realized to the anode constituting the negative pole of the stack. For an acid electrolyte, it can be written:



while the electrochemical reduction of oxygen occurs with a catalytic cathode, constituting the positive pole of the cell:



The e.m.f. stack E is equal to the difference of the electrodes voltages (index "c" for cathode and "a" for anode), that is to say:

$$(6) E = E_c^+ - E_a^- .$$

The results of the electrochemical reactions are electrical energy, heat and water as by-product.

The voltage characteristic that means the output voltage versus current (current density), of a single cell can be defined by the following expression (Blunier, *et al.*, 2007):

$$(7) V(j) = E_0 - V_{ohmic} - V_{act} - V_{con} ,$$

where:

- E_0 is the thermodynamic potential of the cell;
- V_{ohmic} is the ohmic voltage drop resulting from the resistances of the conduction protons through the membrane and of the electrons through the electrical circuit;
- V_{act} is the activation overpotential or the voltage drop due to the activation of the anode and cathode;
- V_{con} is the voltage drop, which results from the reduction in concentration of the reactant gases, or from the transport of mass of oxygen and hydrogen.

One of the most known empirical models is the model described by Kim (1995):

$$(8) V(J) = E_0 - b \log(J) - R J - m \exp(n J) ,$$

with V the approximated voltage drop between the cell terminals, J the current density referred to the electrodes and

$$(9) E_0 = E_r + b \log(J_0) .$$

The first three terms of the equation (8) represents the cell potential in the low and intermediate current density region (activation overpotential and ohmic potential).

The coefficients have the following significations:

- E_r is the reversible voltage of the cell;
- J_0 and b are the Tafel parameters for oxygen reduction;
- R is the ohmic resistance (contributions of the membrane resistance, charge-transfer resistance, electronic resistance, mass-transport resistance).

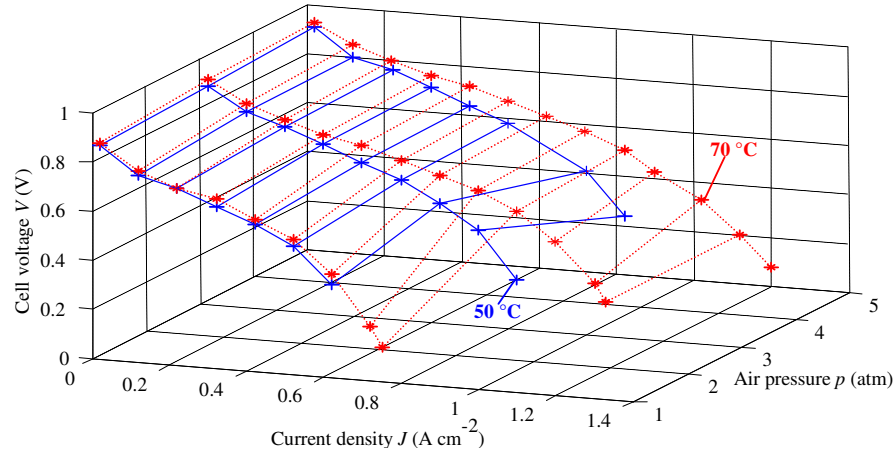


Fig.1. Experimental dataset ('+' at T= 50 °C, '*' at T= 70 °C)

The term $m \cdot \exp(nJ)$ has been introduced to take into account for the mass-transport overpotential as a

As is shown in (Kim, *et al.*, 1995), the equation (1) allows a well fit of the fuel cell characteristic, but imposes the computing of the parameters E_0 , b , R , m and n for specific conditions. This particularity weakens the predictive character of this method.

Thus, a method which allows a well approximation of the fuel cell characteristic and the prediction of the fuel cell performance in a given domain, becomes necessary.

2.2. The MLS method

There are a large number of methods about the functions approximation. The regression models actually represent the most widely spread method exploiting basis functions to fit data. Among these techniques the moving least squares method (MLS), provides both an accurate local function approximation and a continuous gradient approximation (Tirnovan, *et al.*, 2008; Bandler, *et al.*, 2004; Lancaster and Salkauskas, 1981; Belytschko, *et al.*, 1994).

A short presentation of the MLS method is exposed below. Consider the sampled dataset $\{(y_i, \mathbf{x}_i)\}_{i=1..N}$, where:

- $\mathbf{y} = \{y_i\}_{i=1..N} = \{y(\mathbf{x}_i)\}_{i=1..N}$ is the vector of function values in the experimental points;
- $\mathbf{x}_i \in D$ is the vector of the coordinates of the i experimental points, with D the experimental domain containing N samples.

According to MLS, the local character is ensured by a weight function $\delta(\mathbf{x}, \mathbf{x}_i)$ defined on a support region $S(\mathbf{x}_i)$ around \mathbf{x}_i :

function of current density. The coefficients E_0 , b , R , m and n have been determinate using a nonlinear regression method (Kim, *et al.*, 1995).

$$(10) \delta(\mathbf{x}, \mathbf{x}_i) = \delta(\mathbf{x} - \mathbf{x}_i) \begin{cases} \geq 0 & \forall \mathbf{x} \in S(\mathbf{x}_i) \\ = 0 & \text{if not} \end{cases},$$

with \mathbf{x} the vector of the coordinates of a generic point.

This weight function defines a finite domain of influence $S(\mathbf{x}_i) \subset \tilde{D}$, around any experimental point \mathbf{x}_i , where \tilde{D} is the approximation domain.

For every point \mathbf{x} , of the domain \tilde{D} , let $\tilde{y}(\mathbf{x})$ be the moving least squares approximation given by:

$$(11) \tilde{y}(\mathbf{x}) = \sum_{j=1}^n m_j(\mathbf{x}) c_j(\mathbf{x}),$$

where $m_j(\mathbf{x})$ is the j -th basis (generally a monome), n ($n < N$) is the number of the bases, and $c_j(\mathbf{x})$ are the coefficients of each base. The n basis terms form the following m -dimensional vector:

$$(12) \mathbf{p}^T(\mathbf{x}) = \{m_j(\mathbf{x})\}_{j=1..n} \quad n < N.$$

The vector $\mathbf{c}(\mathbf{x}) = [c_1(\mathbf{x}), \dots, c_n(\mathbf{x})]^T$ of the coefficients is obtained by solving a regression problem using the weighted least squares error $E(\mathbf{x})$ for the N sampling points, defined as follows:

$$(13) E(\mathbf{x}) = \sum_{i=1}^N \delta(\mathbf{x} - \mathbf{x}_i) \left[\sum_{j=0}^n m_j(\mathbf{x}_i) c_j(\mathbf{x}) - y_i \right]^2.$$

The minimization of the error $E(\mathbf{x})$ with respect to the coefficients $c_j(\mathbf{x})$ gives:

$$(14) \mathbf{c}(\mathbf{x}) = \mathbf{A}^{-1}(\mathbf{x}) \mathbf{B}(\mathbf{x}) \mathbf{y} ,$$

where the matrix \mathbf{A} and \mathbf{B} are defined by:

$$(15) \mathbf{A}(\mathbf{x}) = \sum_{i=1}^N \delta(\mathbf{x} - \mathbf{x}_i) \mathbf{p}(\mathbf{x}_i) \mathbf{p}^T(\mathbf{x}_i) ,$$

$$(16) \mathbf{B}(\mathbf{x}) = [\delta(\mathbf{x} - \mathbf{x}_1) \mathbf{p}(\mathbf{x}_1) \dots \delta(\mathbf{x} - \mathbf{x}_n) \mathbf{p}(\mathbf{x}_n)] .$$

To guarantee the non-singularity of \mathbf{A} , for a point \mathbf{x} , an adequate support $S(\mathbf{x}_i)$ for each sample point \mathbf{x}_i is needed so that $\delta(\mathbf{x} - \mathbf{x}_i) \neq 0$ for at least m experimental points (Belytschko, *et al.*, 1994).

The expression of the global approximation is

$$(17) \tilde{\mathbf{y}}(\mathbf{x}) = \mathbf{P}^T(\mathbf{x}) \mathbf{A}^{-1}(\mathbf{x}) \mathbf{B}(\mathbf{x}) \mathbf{y} .$$

3. APPLICATION

To ensure the computational feasibility and the accuracy of the application, each point of the approximation domain must be situated in an approximate constant number of supports around the experimental points. Thus an algorithm to compute the optimal support around each sample data has been developed. After pre-processing the experimental data (data have been normalized), the MLS method can be applied to approximate the characteristic of the PEMFC.

To estimate the accuracy of the method, the absolute relative errors have been computed as follow:

$$(18) \bar{\varepsilon}_i = 100 \left| \frac{\tilde{V}(\mathbf{x}_i) - V(\mathbf{x}_i)}{V(\mathbf{x}_i)} \right| (\%),$$

where:

- $\mathbf{x}_i = (J_i, p_i, T_i) \in D$ are the experimental points;
- $V(\mathbf{x}_i) = V_i$ are the experimental values of the cell voltage for the N experiments;
- $\tilde{V}(\mathbf{x}_i) = \tilde{V}_i$ are the approximated values of the cell voltage for the N experimental points.

The average error for all the experimental points is given. The expression of this error is, in percentage:

$$(19) \bar{\varepsilon}_g = \frac{1}{N} \sum_{i=1}^N \bar{\varepsilon}_i ,$$

with N the number of the experimental points.

The computed value of the global relative error is $\bar{\varepsilon}_g = 1.62\%$. Figs 2 and 3 show the approximated fuel cell characteristics in the experimental conditions (temperature, pressure, oxygen excess ratio $S = 2$).

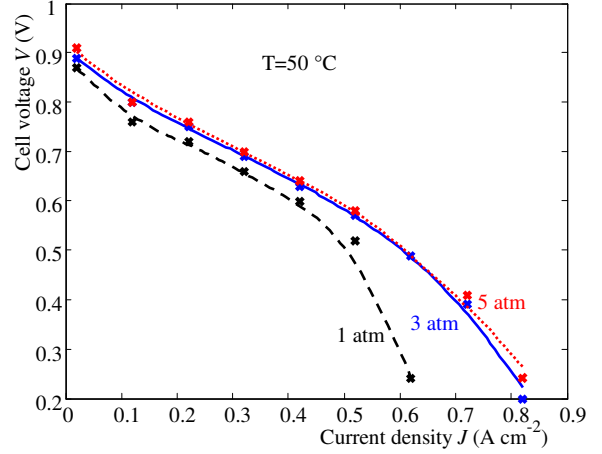


Fig.2. Fuel cell voltage approximated characteristic, at $T = 50$ °C, for three different pressures: 1 atm, 3 atm and 5 atm ('×' experimental data).

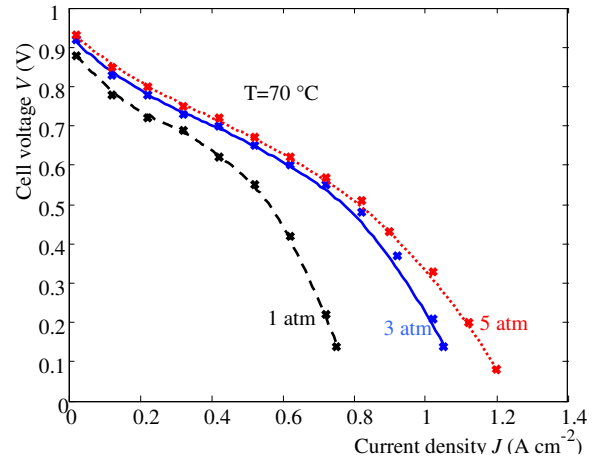


Fig.3. Fuel cell voltage approximated characteristic, at $T = 70$ °C, for three different pressures: 1 atm, 2 atm and 3 atm ('×' experimental data).

However, the true interest of the method is the prediction and the description of the fuel cell behaviour in all of the points of the approximation domain.

Since available data are few, part of the data cannot be kept aside for validation. Thus, the procedure of "cross-validation" (Stone, 1974) is used. This validation procedure can be described as following:

- the experimental dataset is split into T distinct segments;
- then the approximation is executed using data from $T-1$ of the segments and its performance is tested using the remaining segment.

Because the experimental data are poor, in this paper the validation has been practiced in two phases.

3.1. The First Phase of the Method Validation

For the two operating temperatures (50 °C and 70 °C), based on the coefficients computed with all experimental points, another two characteristic, for 2 and 4 atm pressures, have been predicted. Fig. 4 shows the approximated results for the five operating air pressures 1, 2, 3, 4, 5 atm at 70 °C fuel cell temperature.

Now 40 new points (20 for 50 °C temperature and the others 20 for 70 °C temperature), which have been obtained from the approximated results for 2 atm and 4 atm, have been added at the initial dataset.

Then the approximation method has been applied on this new "experimental" domain.

To realise the "cross-validation" another experiment is performed by excluding experimental points corresponding at the 3 atm pressure. Starting from this reduced experimental domain, the characteristic curves have been reconstructed. This reconstruction includes the curves corresponding to the excluded points. Fig.5 shows the approximated results obtained by the exclusion of the experimental real points for the 3 atm pressure.

An analysis of the relative errors for each analyzed point ($i=1\dots 12$) has been performed. In Table 1, $\bar{\epsilon}_{1,i}|_{i=1\dots 12}$ are the absolute relative errors computed for the first case (all experimental points take into account) and $\bar{\epsilon}_{2,i}|_{i=1\dots 12}$ are the absolute relative errors computed in the second case (exclusion of the experimental real points corresponding at the 3 atm operation pressure). The difference between the errors:

$$(20) \Delta \bar{\epsilon}_{1-2,i}|_{i=1\dots 12} = \bar{\epsilon}_{1,i}|_{i=1\dots 12} - \bar{\epsilon}_{2,i}|_{i=1\dots 12}$$

and the average error in each case, have been computed. These show that the method can be used to predict the behaviour of the cell in the entire experimental domain with a good accuracy.

Fig. 6 describes the results of the approximation method for several V - J fuel cell characteristic, for different values of the pressure at an operating fuel cell temperature about 70 °C. These graphic representations prove the accuracy of the proposed method.

3.2. The Second Phase of the Method Validation

For the three operating pressures (1 atm, 3 atm and 5 atm), based on the coefficients computed with all experimental points, another three characteristic, for 55 °C, 60 °C and 65 °C temperatures, have been predicted. Fig. 7 shows the approximated results for the five operating fuel cell temperatures 50, 55, 60, 65 and 70 °C at 3 atm air pressure. Now 90 new

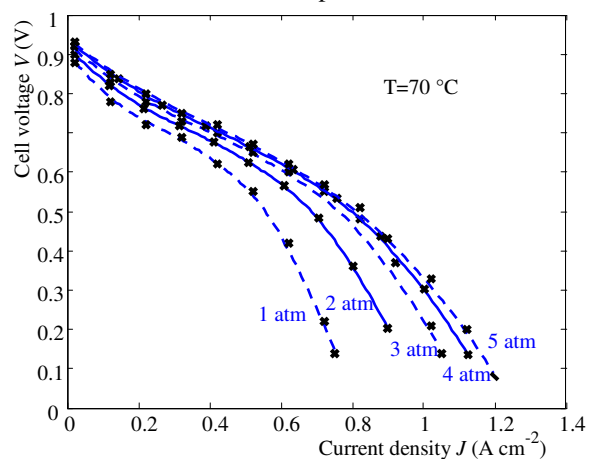


Fig.4. Fuel cell voltage approximated characteristic with predicted data for 2 atm and 4 atm.

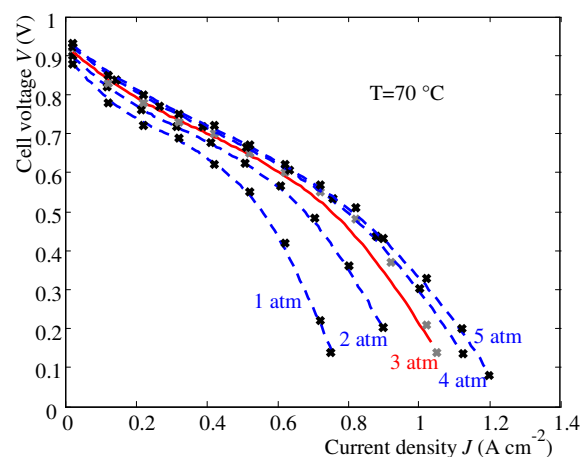


Fig.5. Fuel cell voltage approximated characteristic with the 3 atm data points exclusion.

Table 1 The computed errors for "cross-validation" at 70 °C.

i	J (A cm ⁻²)	$\bar{\epsilon}_1$ (%)	$\bar{\epsilon}_2$ (%)	$\Delta \bar{\epsilon}_{1-2}$ (%)	$\bar{\epsilon}_{g1}$ (%)	$\bar{\epsilon}_{g2}$ (%)
1	0.02	0.78	1.02	-0.24	3.23	3.75
2	0.12	1.30	1.26	+0.04		
3	0.22	0.28	0.26	+0.02		
4	0.32	0.71	0.67	+0.04		
5	0.42	1.0	1.11	-0.11		
6	0.52	0.45	0.63	-0.18		
7	0.62	0.88	1.27	-0.39		
8	0.72	3.36	4.36	-1.0		
9	0.82	7.15	9.07	-1.92		
10	0.92	10.66	13.30	-2.64		
11	1.02	9.07	12.04	-2.97		
12	1.05	3.12	0.6	+2.52		

points which have been obtained from the approximated results for 55 °C, 60 °C and 65 °C, have been added at the initial dataset. Then the approximation method has been applied on this new "experimental" domain.

To accomplish the validation another experiment

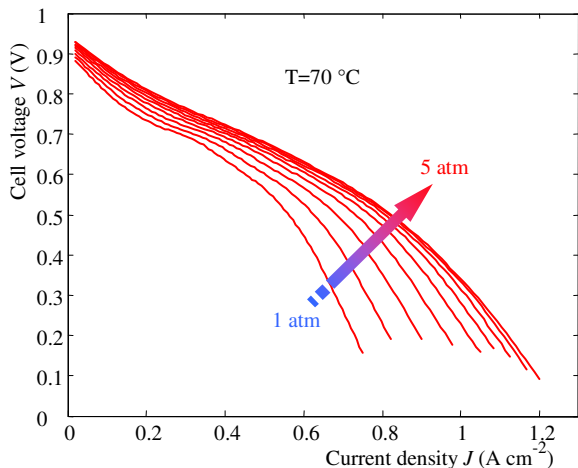


Fig.6. Fuel cell voltage predicted characteristic, at T=70 °C, for several pressures.

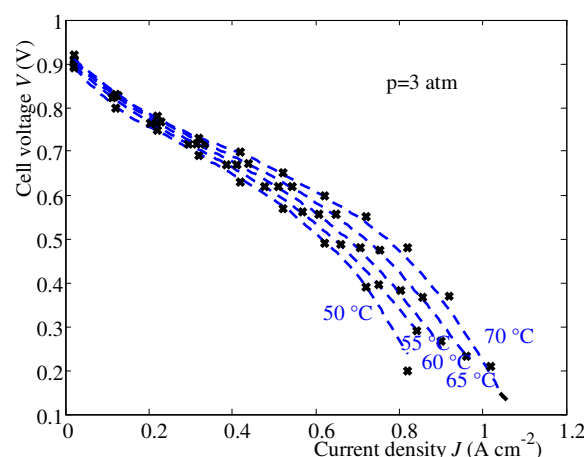


Fig.7. Fuel cell voltage approximated characteristic with predicted data for 55 °C, 60 °C and 65 °C.

has been performed by excluding the experimental points corresponding at the 60 °C operating fuel cell temperature.

Starting from this reduced experimental domain, the characteristic curves have been reconstructed. This reconstruction includes the curves corresponding to the excluded points. Fig. 8 shows the approximated results obtained by the exclusion of the experimental real points for the 60 °C operating fuel cell temperature.

An analysis of the relative errors for each analyzed point ($i=1\dots 10$) has been executed. In Table 2

$\bar{\epsilon}_{3,i}|_{i=1\dots 12}$ are the absolute relative errors computed for the first case (all "experimental" points take into account) and $\bar{\epsilon}_{4,i}|_{i=1\dots 12}$ the absolute relative errors computed in the second case (exclusion of the generated points corresponding at the 60 °C operating fuel cell temperature). The difference between the errors

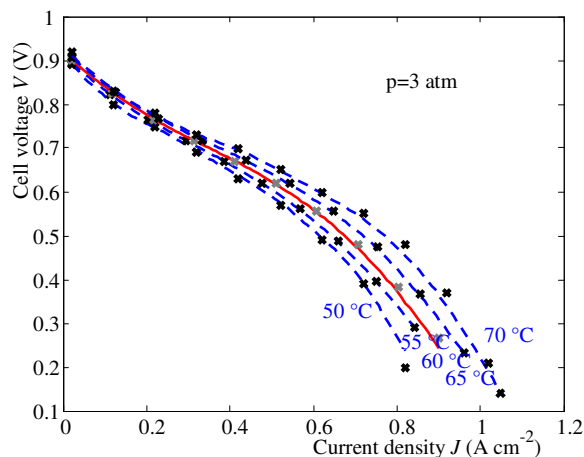


Fig.8. Fuel cell voltage approximated characteristic with the 60 °C data points exclusion.

Table 2 The computed errors for "cross-validation" at 3 atm.

i	J (A cm ⁻²)	$\bar{\epsilon}_3$ (%)	$\bar{\epsilon}_4$ (%)	$\Delta\bar{\epsilon}_{3-4}$ (%)	$\bar{\epsilon}_{g3}$ (%)	$\bar{\epsilon}_{g4}$ (%)
1	0.02	0.7	0.12	+0.58	1.17	1.60
2	0.118	0.38	0.38	0		
3	0.215	0.23	0.22	+0.01		
4	0.314	0.08	0.09	-0.01		
5	0.418	0.06	0.008	+0.052		
6	0.51	0.027	0.24	-0.213		
7	0.607	0.057	0.64	-0.583		
8	0.705	1.28	1.60	-0.32		
9	0.803	2.69	3.83	-1.14		
10	0.901	6.06	8.83	-2.77		

$$(21) \Delta\bar{\epsilon}_{3-4,i}|_{i=1\dots 12} = \bar{\epsilon}_{3,i}|_{i=1\dots 12} - \bar{\epsilon}_{4,i}|_{i=1\dots 12},$$

and the average error in each case, have been computed. This experiment shows that the method can be used to predict the behaviour of the cell in the entire experimental domain with a good accuracy.

4. CONCLUSION

Many mathematical models of fuel cells have been developed either from a theoretical point of view, either from an empirical point of view.

This paper proposes and develops a numerical method for modelling fuel cells based on moving least squares (MLS). The use of MLS is justified by the fact that it is a powerful method for

approximating a function when few data are available, as in the case under study. The proposed model belongs to the family of "black-box" models.

In conclusion, it can be said that:

- the proposed methodology is suitable for modelling PEMFC starting from rare experimental dataset;
- the validation of the method has been performed using the procedure of "cross-validation". It is based on the graphical results and relative errors estimation. The level of the relative errors shows the accuracy of this approach;
- the method can be improved to obtain a better precision in the neighbourhood of the domain boundary by adjusting the compact supports associated to the experimental points;
- the PEMFC characteristics can be predicted and used for the development of the global model of the fuel cell system;
- the method can be applied for modelling another fuel cell power source sub-systems, such as the compression sub-system (compressor);
- the method can be used for off-line or on-line identification of the fuel cell stack.

Stone, T.M. (1974), Cross-validated choice and assessment of statistical predictions, *J. Royal Statist. Society B*, 36 (1974) 111-147.

Tirnovan, R., Giurgea, S., Miraoui, A., Cirrincione, M. (2008). Surrogate model for proton exchange membrane fuel cell (PEMFC), *J. of Power Sources* 175 (2008) 773-778.

5. REFERENCES

- Bandler, J.W., Cheng, Q.S., Dakrouy, A.S., Mohamed, A.S., Bakr, M.H., Madsen K. and Søndergaard, J. (2004). Space mapping: The state of the art, *IEEE Transactions on Microwave Theory and Techniques*, 52 (2004) pp 337-360.
- Belytschko, T., Lu, Y., Gu, L (1994). Element-free Galerkin methods, *International Journal for Numerical Methods in Engineering*, 37 (1994) 229-256.
- Blunier, B., and Miraoui, A. (2007). *Fuel cells, Principle, Modeling and Applications with Exercises and Corrected Problems*, Technosup. France, 2007.
- Cheddie, D., and Munroe, N. (2005). Review and comparison of approaches to proton exchange membrane fuel cell modelling, *J. of Power Sources*, 147 (2005) 72-84.
- Cogeneration & On-Site Power Production, 8, Issue 1 January / February 2007, News.
- Kim, J., Lee, S. Srinivasan, S., Chamberlin, and Ch.E. (1995). Modeling of proton exchange membrane fuel cell performance with an empirical equation, *J. Electrochem. Soc.*, 142, No. 8 (1995) 2670-2674.
- Lancaster, P., and Salkauskas, K. (1991). Surfaces generated by moving least squares methods, *Mathematics of Computation*, 37, No. 155, Academic Press Inc., 1981, pp 141-158.